DESIGN AND ANALYSIS OF VIBRATORY SCREEN FOR PEANUTS

by

Emre KAYGUSUZ*

Pilot University of Central Coordination Unit, Bingol University, Bingol, Turkiye

Original scientific paper
https://doi.org/10.2298/TSCI2304323K

The low-cost cleaning and classification of granular agricultural products in a vibrating environment is possible via the mathematical modeling of the movement of a grain on the surface of the screen. In this study, design and analysis of a vibratory screen used for cleaning and classifying peanuts has been realized. Therefore, firstly a mathematical model of this process has been developed based on analysis carried out on a grain making translation on a vibrating surface. A 6-bar mechanism was selected as the driving system and the kinematical analysis was performed to obtain the basic inputs of the vibratory screen. Based on the mathematical model developed, a design algorithm has been formed by which design and operating parameters are selected so as to satisfy the necessary conditions for effective sieving. This way ensures saving money and time. The algorithm has been demonstrated on a numerical example and it is shown suitable to sieve the peanut.

Key words: *vibratory screen, design, mathematical model, sieve peanut, mechanism*

Introduction

Separation of agricultural products is one of the major post-harvest processes employed for cleaning and grading to ensure standardization for sale and/or manufacturing practices. Particulate agricultural products could be separated by employing their physical properties such as color, blemish, shape, size, weight, density, *etc.* Sizing is one of the major separation processes for cleaning debris and grading granular materials using measurable dimensions.

Many and various types of screening mechanisms are used in cleaning and sizing of agro-products such as flat and reel vibrating screeners [1-6]. Among these mechanisms, the vibratory screen has been widely used [1]. Vibrating screen is one of the most important machines used extensively in order to categorize the product.

There are a lot of sifting factors which affect to screening. However, the major sifting factor is vibration motion. Vibration motion has defined frequency and amplitude of vibration and direction of vibration motion. It is very important because election performance of screen depends on screen vibration [7-11].

Cleaning and grading of particulate products according to size is extensively achieved using vibratory screens. The major factor governing the efficiency of a vibratory screen is the vibration motion defined by the parameters of frequency, amplitude and direction of the vibration. Efficiency of vibratory screens is modeled analytically [12], empirically

* Author's, e-mail: emrekaygusuz@bingol.edu.tr

[13, 14], and numerically using simulation programs [15-17]. The real time experimental test is the very final step, because of the high cost, in current design works for justifying the model.

There are new studies and types designs of vibratory screens used for mining, named vibrating flip-flow screens (VFFS) and single-body circular vibrating screen (CVS) [18]. Yu *et al*. [18] said that VFFS screening performance was better then CVS.

Modrzewski *et al.* [19], suggested double frequency vibrators on screens and analyzed their dynamical behaviour. Researchers formulated high complexity vibration frequencies of vibratory screens [19].

Chen *et al*. [20] investiged elliptical vibratory screen for industrial application and applied numerical analyses. The screening parameters and performance of the vibrating screen are set forth for future research and development activities [20].

In this study, kinematic analysis of the selected 6-bar sieve drive mechanism was used to calculate effective acceleration components on the sieve surface. The mathematical model of the relative motion of the peanut according to the sieve surface was obtained with the effect of acceleration components. A design algorithm has been developed that includes the mathematical model and the elimination index. The algorithm is converted to Pascal language. Thus, numerical experiments have been made effectively by changing systematically the operation and dimension parameters in the computer program. Based on the numerical results, the design process has been completed by determining the elimination parameters that make the elimination index the best. As a result, the vibratory screen is theoretically, designed, analyzed, manufactured and tested.

Material and methods

Formulation of the problem

In vibratory screens, the separation takes place on a planar screen of perforated steel or woven wire in general. Particles with smaller sizes than those of meshes of the screen fall through the mesh openings due to gravitational force. Particles remaining on the surface are moved forward along with the screen. During the motion, particles are under the effect three major forces, namely the normal force between the particle and screen surface, friction force resisting the motion of the particle and the weight of the particle. In order to control the screening, it is necessary to know the relative motion of the product under gravity effect.

Motion of the grain on the screen

The motion of the particle along screen must be analyzed relative to the screen itself. Let a grain with mass of m be moving on the surface of a screen with the screen slope of δ, accelerations of a_{ex} and a_{ey} in the x- and y-axes, respectively and the coefficient of kinematic friction of μ, figs. 1 and 2.

For an efficient separation, the particle is supposed to have no relative motion in the y-direction. In other words, the grain velocity, V_{ey}, and acceleration, a_{ey}, should be equal to those of the screen in the y-direction. The relative motion is supposed to be only in the x-direction. Under the given conditions, according to Newton's Second Law:

$$N = m(a_{ey} + g\cos\delta) \tag{1}$$

$$a_{fx} = -g\sin\delta - \mathrm{Sgn}(V_{fex})\mu(a_{ey} + g\cos\delta) \tag{2}$$

where N is the normal force, a_{fx} – the is absolute grain acceleration in the x-direction, g – the gravitational acceleration, V_{fex} – the relative velocity of the particle with respect to the screen, and $Sgn(V_{fex})$ – a sign function:

$$\mathrm{Sgn}\,(V_{fex}) = \begin{cases} 1 & V_{fex} > 0 \\ -1 & V_{fex} < 0 \end{cases} \tag{3}$$

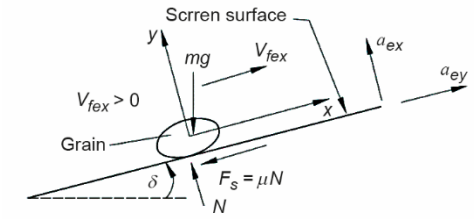

Figure 1. Upwards relative motion

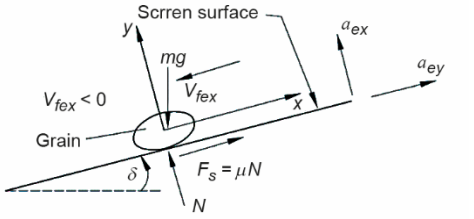

Figure 2. Downwards relative motion

Then, the particle relative acceleration, a_{fex}, the grain relative velocity, V_{fex}, and the relative displacement in the x-direction, S_{fex}, become:

$$a_{fex} = -\mathrm{g}\sin\delta - \mathrm{Sgn}(V_{fex})\mu(a_{ey} + \mathrm{g}\cos\delta) - a_{ex} \tag{4}$$

$$V_{fex} = \int_{t_{i-1}}^{t_i} a_{fex}\,\mathrm{d}t, \quad t_i = t_{i-1} + h, \quad i = 1,...,n \tag{5}$$

$$S_{fex} = \int_{t_{i-1}}^{t_i} V_{fex}\,\mathrm{d}t, \quad t_i = t_{i-1} + h, \quad i = 1,...,n \tag{6}$$

where, t_i, t_{i-1} are consecutive times separated by increment of h.

The initial condition can be written:

$$\left.\begin{aligned} |a_{fex} &= 0 \\ |V_{fex} &= 0 \\ |S_{fex} &= 0 \end{aligned}\right\} t_0 = 0 \tag{7}$$

For the separation to take place, N should be larger than zero, eq. (1), for the particle to be contact ever with the screen, and expressed mathematically by:

$$a_{ey} \geq -\mathrm{g}\cos(\delta) \tag{8}$$

Another condition is the existence of relative motion of the grain in the x-direction. If at any time $V_{fex} = 0$, a_{ex} must overcome the friction force between the particle and the screen defined by:

$$\mathrm{Abs}(a_{ex}) \geq \mathrm{Abs}[\mathrm{g}\sin\delta + \mathrm{Sgn}(a_{ex})\mu(a_{ey} + \mathrm{g}\cos\delta)] \tag{9}$$

Screening conditions

The possible relative motion of the particle with respect to the screen and its possible position with respect to the mesh is depicted in figs. 3(a) and 3(b).

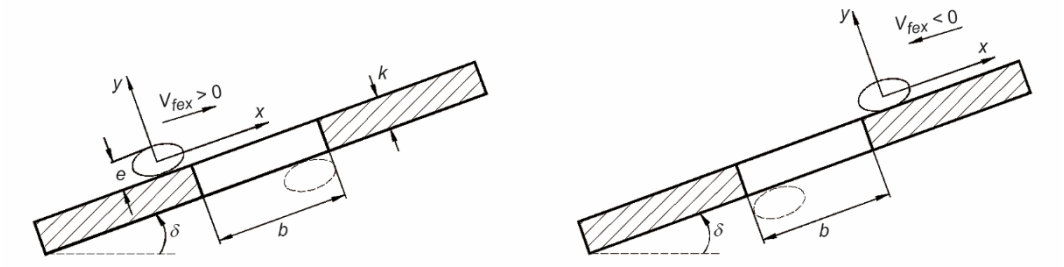

Figure 3. Screening conditions; (a) upwards relative motion and (b) downwards relative motion

Accordingly, the initial condition for the motion:

$$x(0) = 0$$

$$y(0) = 0$$

$$\left.\frac{\mathrm{d}x}{\mathrm{d}t}\right|_{t=0} = V_{fex}$$

$$\left.\frac{\mathrm{d}y}{\mathrm{d}t}\right|_{t=0} = 0 \tag{10}$$

Then the position of the grain is expressed by:

$$x(t) = -\frac{1}{2}\mathrm{g}\sin\delta t^2 + V_{fex}t \tag{11}$$

$$y(t) = -\frac{1}{2}\mathrm{g}\cos\delta t^2 \tag{12}$$

For the grain to pass through the mesh:

$$0 \geq y \geq -k - e, \quad 0 < x \leq b \tag{13}$$

where k is the screen thickness, e – the thickness of the grain, and b – the mesh length.

Considering the position of the grain, eqs. (11) and (12), and the limiting condition in eq. (13) the critical speed is obtained:

$$V_{fex} = [b + \mathrm{g}\tan\delta(k+e)]\sqrt{\frac{\mathrm{g}\cos\delta}{2(k+e)}} \tag{14}$$

In the case of downward motion of the grain, fig. 3(b), the following limiting condition is in effect:

$$0 > x \geq -b \tag{15}$$

Accordingly, relative downward velocity is:

$$V_{fex} = [-b + \mathrm{g}\tan\delta(k+e)]\sqrt{\frac{\mathrm{g}\cos\delta}{2(k+e)}} \tag{16}$$

Determination of screen acceleration

Many various mechanisms can be used to drive the screen. In this work 6-bar mechanism, fig. 4, is selected as the screen driving mechanism. Screen of acceleration component is presented on fig. 5.

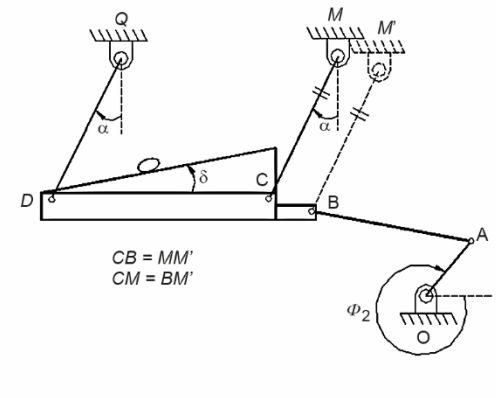

Figure 4. Screening drive system

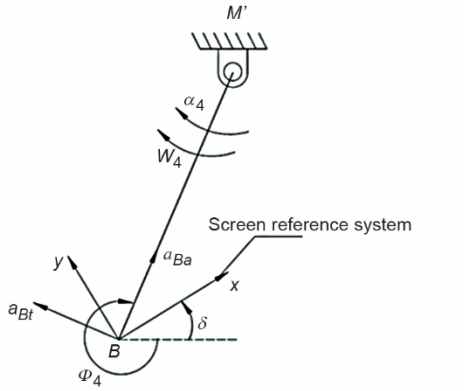

Figure 5. Screen acceleration component

For the kinematic analysis of the system, if the DCMQ four-bar mechanism is selected as a parallelogram linkage, the analysis is reduced to OABM four-bar mechanism, fig. 6.

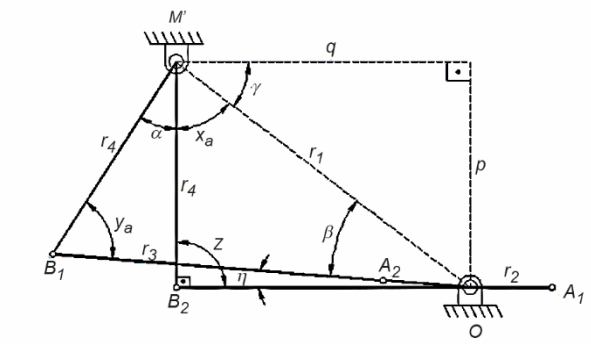

Figure 6. Simplified 4-bar mechanism

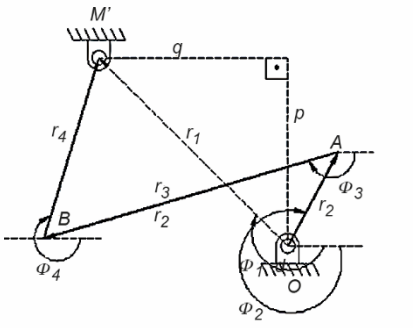

Figure 7. Screen drive system position

The 4-bar mechanism functions as a crank-rocker mechanism generating a vibration at an angle of α. With two limiting positions of the crank-rocker, fig. 6, if Sinus theorem is applied within QB1M and QB2M triangles for $p = r4$ and $z = 900$, the crank-rocker mechanism dimensions would be:

$$\frac{r_4}{r_1} = \frac{1}{2}\left[\frac{\sin(\alpha + x_a)}{\sin y_a} + \frac{\sin x_a}{\sin z}\right] \tag{17}$$

$$\frac{r_3}{r_1} = \frac{1}{2}\left[\frac{\sin(\alpha + x_a)}{\sin y_a} - \frac{\sin x_a}{\sin z}\right] \tag{18}$$

where $x_a = 90 - \tan^{-1}(p/q)$, $r_1 = \sqrt{p^2 + q^2}$, $y_a = 180 - (\alpha + x_a + \beta)$.

Then the following loop equation could be written for fig. 7 in the scalar form:

$$\vec{r}_2 + \vec{r}_3 + \vec{r}_4 - \vec{r}_1 = 0 \tag{19}$$

where

$$\Phi_3 = 2\tan^{-1}\left(\frac{-b_1 - \sqrt{b_1^2 - 4a_1c_1}}{2a_1}\right) \tag{20}$$

$$a_1 = r_1^2 + r_2^2 + r_3^2 - r_4^2 - 2r_1r_2\cos(\Phi_2 - \Phi_1) - 2r_2r_3\cos\Phi_2 + 2r_1r_3\cos\Phi_1 \tag{21}$$

$$b_1 = 2(2r_2r_3\sin\Phi_2 - 2r_1r_3\sin\Phi_1) \tag{22}$$

$$c_1 = r_1^2 + r_2^2 + r_3^2 - r_4^2 - 2r_1r_2\cos(\Phi_2 - \Phi_1) + 2r_2r_3\cos\Phi_2 - 2r_1r_3\cos\Phi_1 \tag{23}$$

$$\Phi_4 = 2\tan^{-1}\left(\frac{-b_2 + \sqrt{b_2^2 - 4a_2c_2}}{2a_2}\right) \tag{24}$$

$$a_2 = r_1^2 + r_2^2 + r_4^2 - r_3^2 - 2r_1r_2\cos(\Phi_2 - \Phi_1) - 2r_2r_4\cos\Phi_2 + 2r_1r_4\cos\Phi_1 \tag{25}$$

$$b_2 = 2(2r_2r_4\sin\Phi_2 - 2r_1r_4\sin\Phi_1) \tag{26}$$

$$c_2 = r_1^2 + r_2^2 + r_4^2 - r_3^2 - 2r_1r_2\cos(\Phi_2 - \Phi_1) + 2r_2r_4\cos\Phi_2 - 2r_1r_4\cos\Phi_1 \tag{27}$$

Assuming the mechanism input link w_2 rotates with at a constant angular velocity, the first time derivative of eq. (19) with respect to time results in two scalar equations with two unknowns, namely angular speeds of the connecting link, w_3, and output link, w_4:

$$w_3 = w_2\frac{r_2}{r_3}\frac{\sin(\Phi_2 - \Phi_4)}{\sin(\Phi_4 - \Phi_3)} \tag{28}$$

$$w_4 = w_2\frac{r_2}{r_4}\frac{\sin(\Phi_2 - \Phi_3)}{\sin(\Phi_3 - \Phi_4)} \tag{29}$$

The second derivative of eq. (19) with respect to time gives the acceleration and results in two scalar equations with two unknowns, namely angular acceleration of the connecting link, α_3, and output link, α_4:

$$\alpha_3 = \frac{r_2 w_2^2 \cos(\Phi_4 - \Phi_2) + r_3 w_3^2 \cos s(\Phi_4 - \Phi_3) + r_4 w_4^2}{r_3 \sin(\Phi_4 - \Phi_3)} \tag{30}$$

$$\alpha_4 = \frac{r_2 w_2^2 \cos(\Phi_3 - \Phi_2) + r_4 w_4^2 \cos(\Phi_3 - \Phi_4) + r_3 w_3^2}{r_4 \sin(\Phi_3 - \Phi_4)} \tag{31}$$

Using w_4 and α_4 two components along the axes of the x-y co-ordinate system, fig. 5, is obtained :

$$a_{ex} = w_4^2 r_4 \cos(360° - \Phi_4 - \delta) - \alpha_4 r_4 \cos(270° - \Phi_4 - \delta) \tag{32}$$

$$a_{ey} = w_4^2 r_4 \sin(360° - \Phi_4 - \delta) - \alpha_4 r_4 \sin(270° - \Phi_4 - \delta) \tag{33}$$

Screen design and analysis according to the suitable product motion

The following algorithm developed using the mathematical model was employed for an effective screening design together with the provided parameters through given steps:

1. Basic parameters (p, q, α, z, δ, w_2, μ, n) are entered, where n stands for the number of time increments. Enter the basic parameters (p, q, α, z, δ, w_2, μ, n).
2. Using p, q, α, z and eqs. (17) and (18), the fixed body position angle, Φ_1, and link lengths (r_1, r_2, r_3, r_4) are determined.
3. The time increment is found through $T = 2\pi/w_2$ and $h = T/n$, (T is cycle period of the screen).
4. At the start of the motion $t_0 = 0$ is taken for $i = 0$.
5. Time is get run by $t_i = t_i - 1 + h$.
6. The crank angle is computed through $\Phi_{2i} = w_2 h(i - 1)$ for $t = t_i$.
7. Connecting and output link, Φ_{3i}, Φ_{4i}, are determined using eqs. (20) and (24) for $t = t_i$.
8. Angular velocities, w_{3i}, w_{4i}, are computed using eqs. (28) and (29) for $t = t_i$.
9. Angular acceleration, α_{4i}, is determined using eq. (31).
10. Screen drive acceleration components, a_{exi}, a_{eyi}, are calculated using eqs. (32) and (33) for $t = t_i$.
11. If eq. (8) does not work, indicating bouncing, Step 20 is executed.
12. The N_i/m is calculated for $a_{fyi} = a_{eyi}$ using eq. (1) for $t = t_i$.
13. If $i \neq 1$ and $t_0 \neq 0$, Step 15 is executed.
14. The a_{fxi} is set equal to a_{exi}, for initial conditions of $a_{fexi} = 0$, $V_{fexi} = 0$, $S_{fexi} = 0$ and for $t = t_i$.
15. If Step No. 8 does not work for $V_{fexi} - 1 = 0$ and $t = t_i$, Step 20 is executed.
16. If $A_{bs}(V_{fexi} - 1) \neq 0$ or $A_{bs}(V_{fexi} - 1) = 0$ and Step 8 works, the following calculations are carried out:

$$a_{fxi} = -\mathrm{Sgn}(V_{fexi-1})\mu \frac{N_i}{m} - g\sin\delta \tag{32}$$

$$a_{fexi} = a_{fxi} - a_{exi} \tag{33}$$

$$V_{fexi} = (a_{fexi} + a_{fexi-1})\frac{h}{2} + V_{fexi-1} \text{ (trapezoidal rule)} \tag{34}$$

17. If Sgn(V_{fexi}) = Sgn(V_{fexi-1}) Step 19 is executed.
18. The following calculations are executed for a_{fxi}, a_{fexi} and V_{fexi}:

$$a_{fxi} = -\text{Sgn}(V_{fexi})\mu\frac{N_i}{m} - g\sin\delta \tag{35}$$

$$a_{fexi} = a_{fxi} - a_{exi} \tag{36}$$

$$V_{fexi} = (a_{fexi} + a_{fexi-1})\frac{h}{2} + V_{fexi-1} \tag{37}$$

19. Relative displacement is calculated using:

$$S_{fexi} = (V_{fexi} + V_{fexi-1})\frac{h}{2} + S_{fexi-1} \tag{38}$$

20. The *i* is increased by 1 and the loop is restarted again executing Step 5 till the maximum value of i is reached.

Criteria for screening

The previous algorithm provides a method for calculating the relative acceleration, relative velocity and relative displacement of the grain with respect to the screen surface using given input parameters. In assessing the relative motion of the grain on the screen, a criterion called index of screening efficiency, *e*, is taken into account.

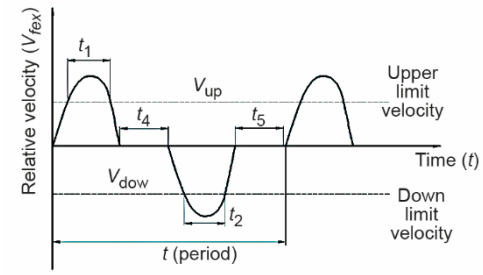

Figure 8. Possible relative velocity of the product on the screen

The *e* is determined using fig. 8 which shows variation of the relative velocity, V_{fex}, of the grain *vs.* time. Screening does not take place through time periods of t_1 and t_2, since the grain velocity beyond the limiting relative velocity. The same way it does not happen through time periods of t_4 and t_5, since the grain relative velocity is zero.

The screening would be effective for $t_3 = T - (t_1 + t_2 + t_4 + t_5)$, thus the ratio giving the period through the screening is effective to the cycle period of the screen, ε:

$$\varepsilon = \frac{t_3}{T} = 1 - \frac{t_1 + t_2 + t_4 + t_5}{T} \tag{39}$$

The average relative velocity of the grain, V_{fexav}, given in eq. (5) is determined from:

$$V_{fexav} = \frac{\int_0^T |V_{fex}|\,\mathrm{d}t}{T} \tag{40}$$

So, the index of screening efficiency, *e*, can be defined:

$$e = \varepsilon V_{fexav} \tag{41}$$

Accordingly, the efficiency of the screening practically gets larger with increasing *e*.

Results and discussion

The previously provided analysis and design algorithm presents assessable conclusions under the light of suitable designing criteria. Setting up an example for this, the application incident to peanut will be demonstrated. The algorithm in question has been converted into a computer software program to allow the analysis of relative acceleration, velocity and displacement values within the two cycles of the screen. The input parameters of the program and effective parameters in screening are the same. The change within the first two cycles of relative velocity and relative displacement obtained from changing of input parameters systematically and the changing of screening index with respect to the effective parameters in screening are developed into graphs. With the application of designing criteria suitable to these graphics, an optimum screen design will have been suggested.

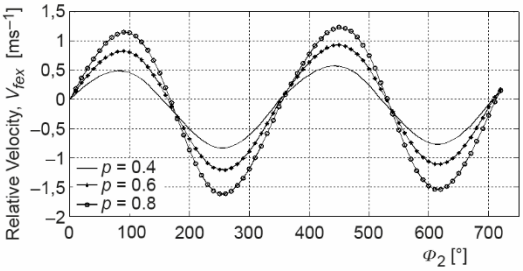

Figure 9. Screen arm length effect on relative velocity

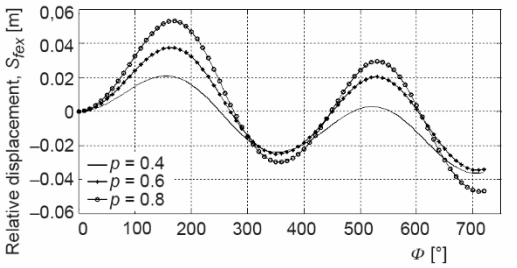

Figure 10. Screen arm length effect on relative path

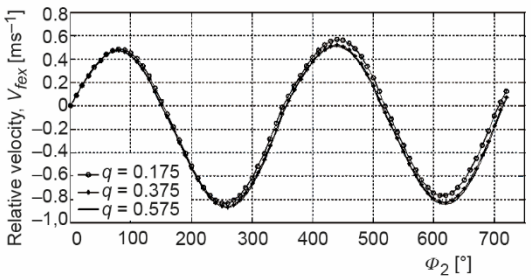

Figure 11. Fixed joint place effect on relative velocity

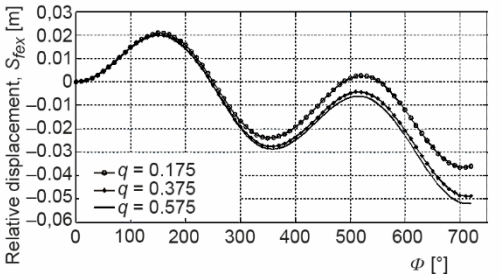

Figure 12. Fixed joint place effect on relative path

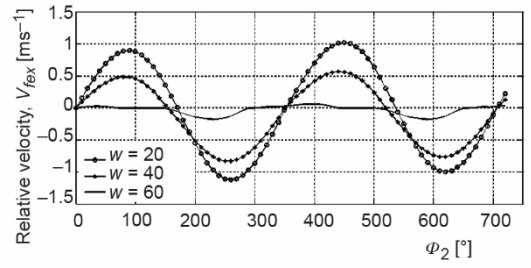

Figure 13. Crank angular velocity effect on relative velocity

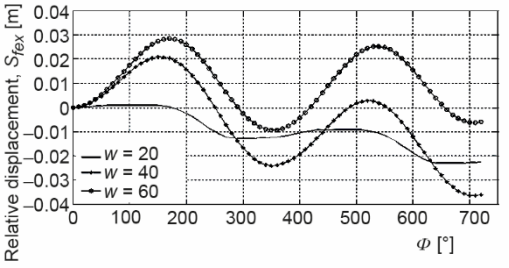

Figure 14. Crank angular velocity effect on relative path

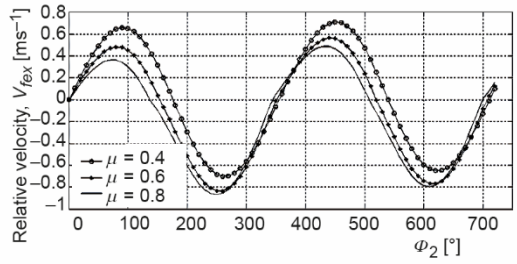

Figure 15. Friction coefficient effect on relative velocity

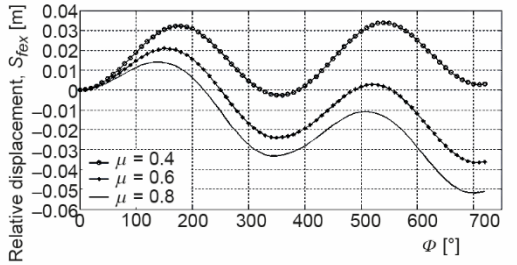

Figure 16. Friction coefficient effect on r elative path

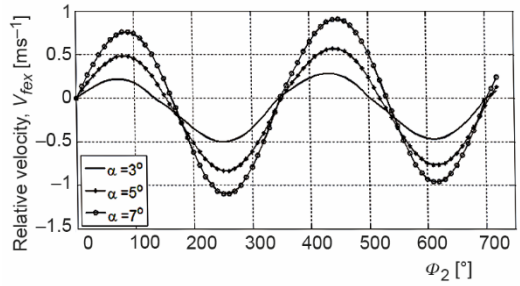

Figure 17. Vibration angle effect on relative velocity

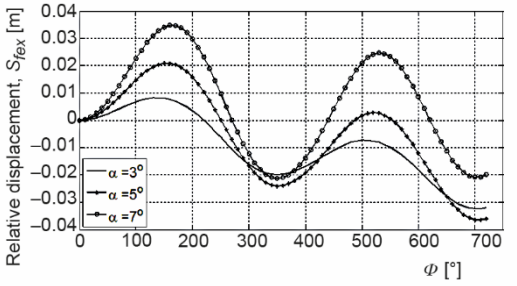

Figure 18. Vibration angle effect on relative path

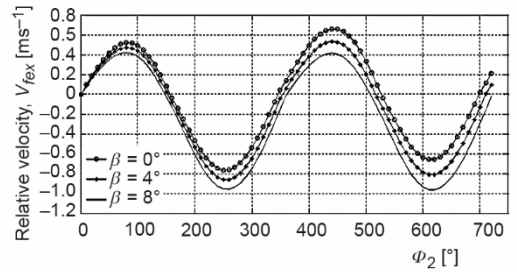

Figure 19. Screen slope angle effect on relative velocity

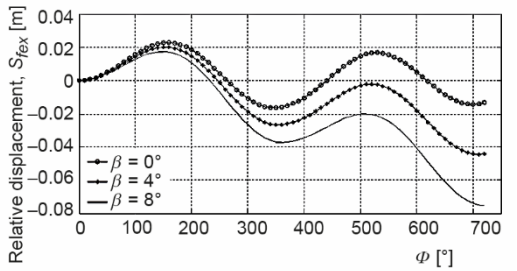

Figure 20. Screen slope angle effect on relative path

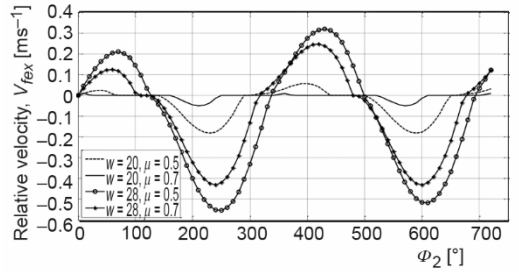

Figure 21. Seed and shell graphic to the relative velocity

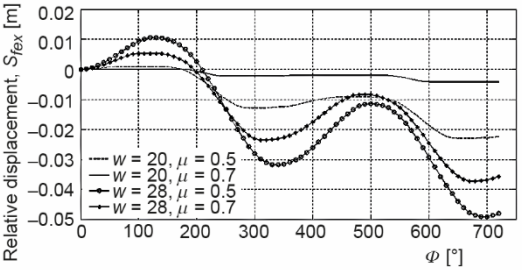

Figure 22. Seed and shell graphic to the relative path

Here, apart from the aforementioned input parameters, the constant magnitudes selected as inputs are as follows:

Screen plate hole diameter b = 20 mm, screen plate thickness k = 1 mm, the average thickness for peanut e = 6 mm.

The numerical values of input parameters about which researches were carried out in all graphics, *except the ones with altered parameters* are selected as below.

p = 400 mm; q = 157.5 mm; α = 50; z = 900; δ = 30; w_2 = 40 *r*/*s*; μ = 0.5; n = 720 number

The dimensions of the crank-rocker mechanism concluded in accordance with this data are:

$$r_1 = 438.6 \text{ mm}; \; r_2 = 17.4 \text{ mm}; \; r_3 = 174.9 \text{ mm}; \; r_4 = 400.0 \text{ mm}$$

The relative velocity, V_{fex}, and relative displacement, S_{fex} of peanut over screen are drawn into graphs. In the earlier graphs, figs. 9 and 10, with the research of p, it is observed that with increase of p values, the magnitude of relative velocity and the relative displacement rise up. Moreover, from fig. 23, with the increase of p, screening index increases rapidly but after p = 400 mm reduction may be observed. As a conclusion, the selection of p large causes difficulty to the screening process. For q with respect to figs. 11, 12, and 23, it is possible to say that the relative velocity, the relative displacement and screening index are not much effected. This provides freedom of choice to the designer in selecting q. In the low values (about w_2 = 20 *r*/*s*) of w_2 drive link angular velocity which is one of the operational parameters, it is observed from figs. 13 and 14 that the peanut from time to time remains still and motionless on the screen, while the grain jumps on the screen in case of higher values (about w_2 = 70 *r*/*s*). As it could be observed in fig. 23, angular velocity has a significant effect on the screening index as well. This situation shows that the angular velocity should be selected among the specific limit values. From figs. 15 and 16 the effects of the friction coefficient, μ, between the screen and the product can be discussed. Observing that in fig. 15, the friction coefficient effect is not effective at an essential degree in the relative velocity, it is seen that it generates a retarding effect in the relative motion as in fig. 16. Moreover, it can be observed, from fig. 23, that the screening index is not excessively effected after 0.2 value of the friction coefficient. This refers to the necessity of taking some precautions in the other parameters against the probable negative effects of friction coefficient arising from screening of different products. Effects of oscillation angle α are demonstrated in the curves of figs. 17 and 18. In the event the curves are examined, as higher as the α value as higher the relative velocity and relative displacement amplitude. Apart from this, it can be observed that with the increase of α parameter, screening index will increase rapidly and reduce after α = 60 as in fig. 23. Since this situation will be negatively effecting the screening, α should be selected carefully.

For the systems where adjustment possibilities exist, one of the variants which can be considered among the operational parameters is the δ angle showing the screen inclination. In fig. 23 a slowly reduction of screening index is observed when the δ increases. Whereas, in figs. 19 and 20 even though little amount of δ is seen to have increasing effects on relative velocity and relative displacement. However, the increases in the δ, shows that the peanuts have taken greater displacement on the screen. As a result, it could be suggested that it is an advantage for the sake of an efficient screening that the screen makes an amount of angle with the horizon.

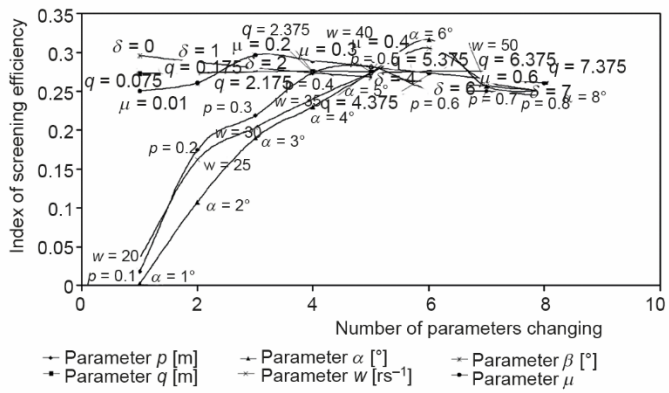

Figure 23. Variation of screening index at efficient parameters at screening

From the general evaluation of the graphs, the operation revolution needs to be selected greater than, w_2, 20 *r*/*s* and smaller than 40 *r*/*s*, the oscillation angle about, α 50, while the existing volume and space restrictions of q taken into consideration are freely selected. Selecting p = 400 mm, screen slope angle, δ, about between 30 to 50 can be concluded to be suitable for an efficient screening.

From the previous observations, the dimensions and operational revolutions of a screen installed to a peanut breaking machine are selected. Considering, the screen parameters, friction coefficient of the shell, the angular velocity which is determined by electric motor and number of revolutions. Optimum design parameters can be developed by computer programs.

The relative velocity and relative displacement of the peanut seed and shell are shown in figs. 21 and 22. As seen in both graphs, it is observed that for the low revolution and low friction coefficients causes the difficult screening. So, it will not be a mistake to say that over reducing operating revolution causes seed and shell to accumulate, while over increasing of revolution will lead to the removal of screening.

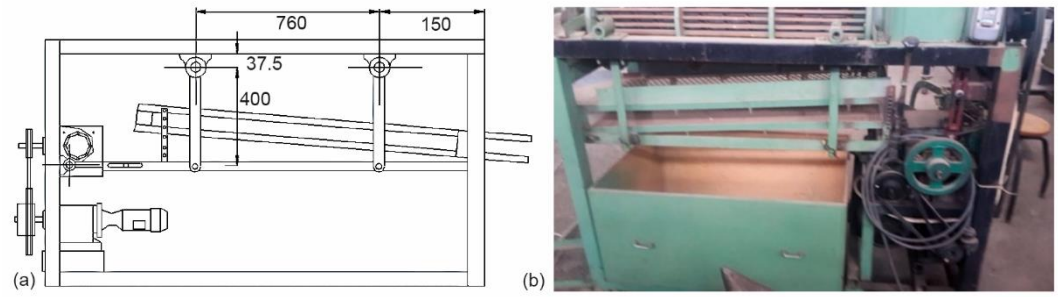

Figure 24. Manufactured vibratory screen model; (a) drawing of model and (b) photo of model

Conclusion

In this study an algorithm has been developed for the designing of a vibratory screen that could provide the separation of the seed and shells of the peanuts. With the assistance of this algorithm, a screen model being designed to realize specific screening criteria and the screen was built under laboratory conditions, fig. 24. In the tests carried out on the manufac-

tured screen, it is observed that the grains moving on the screen are in conformity with the motion emerged in the result of the theoretical examination.

References

[1] Mutaf, E., *Grain Cleaning and Size Grading Machinery*, Ege University Publications, Izmir, Turkiye, 1961
[2] Blankenship, P. D., *et al*., Foreign Material Extractors for Peanut Flowpipes, *Peanut Science*, *11* (1984), 1, pp. 10-12
[3] Dickens, J. W., Screening Viriginia-Type Farmers Stock Peanuts Before Stroge, *Peanut Science*, *11* (1984), 1, pp. 13-16
[4] Nicholls, C. F., Glassman, S. B., A Portable Bean Size Grader, *Canadian Agricultural Engineering*, *27* (1985), 1, pp. 55-57
[5] Hennig, M., Teipel, U., Grade Efficiency for Sieve Classification Processes, *Canadian Journal of Chemical Engineering*, *96* (2018), pp. 259-264
[6] Akcali, I. D., Mutlu, H., Cylinder Internal Helix Screen Designing, *Proceedings*, 4. National Machinery Designing and Manufacturing Congress, METU, Ankara, 1990, pp. 443-454
[7] Fellows, P., *Food Processing Technology: Principles and Practice*, Cambridge, England, 2009, pp. 87
[8] Grandisaon, A. S., *Postharvest Handling an Preparation of Food Processing*, (ed. J. G. Brennan), Willey, New York, USA, 2006
[9] He, X. M., Liu C. S., Dynamics and Screening Characteristics of a Vibrating Screen with Variable Elliptical Trace, *Mining Science and Technology*, *19* (2009), 4, pp. 508-513
[10] Baragetti, S., Innovative Structural Solution for Heavy Loaded Vibrating Screens, *Minerals Engineering*, *84* (2015), Dec., pp. 15-26
[11] Stoicovici, D. I., *et al*., Conputer Model for Sieves' Vibrations Analysis, Using an Algorithm Based on the False-Position Method, *American Journal of Applied Sciences*, *6*, (2009), 1, pp. 48-56
[12] Baragetti, S., Villa, F., A Dynamic Optimization Theoretical Method for Heavy Loaded Vibrating Screens, *Non-linear Dyn*, *78* (2014), 1, pp. 609-627
[13] Kostas, T., Some Basic Factors Affecting Screen Performance in Horizontal Vibrating Screens, *The European Journal of Mineral Processing and Environmental Protection*, (2001), 1, pp. 42-54
[14] Brindeu, L., Ilea, R., Dynamics of the Displacements by Vibrations on Plane Sieves, *Annals of the Faculty of Engineering Hunedoara*, (2004), 1, pp. 9-14
[15] Chen, Y., Tong X., Modeling Screening Efficiency with Vibrational Parameters Based on DEM 3D Simulation, *Mining Science and Technology*, *20* (2010), 4, pp. 0615-0620
[16] Dong, K. J., *et al.*, DEM Simulation of Particle Flow on a Multi-Deck Banana Screen, *Minerals Engineering*, *22* (2009), 11, pp. 910-920
[17] Mossneguttu E., *et al*., Influence of Screening Block Supporting Way On The Behaviour of A Solid Particle On an Oscillating Surface, *Journal of Engineering Studies and Research*, *21* (2015), 3, pp. 51-58
[18] Yu, C., *et al*., Comparison of Flip-Flow Screen and Circular Vibrating Screen Vibratory Sieving Processes for Sticky Fine Particles, *Minerals Engineering*, *187* (2022), Sept., 107791
[19] Modrzewski, R., *et al.*, A Study on the Dynamic Behavior of a Sieve in an Industrial Sifter, *Applied Sciences*, *12* (2022), 17, 8590
[20] Chen, Z., *et al.*, Numerical Investigation on the Sieving Performance of Elliptical Vibrating Screen, *Processes*, 8 (2020), 9, 1151

Paper submitted: January 26, 2023
Paper revised: April 19, 2023
Paper accepted: May 16, 2023